J|A|C|S
ARTICLES
Published on Web 02/11/2006

Effect of Antifreeze Proteins on the Nucleation, Growth, and the Memory Effect during Tetrahydrofuran Clathrate Hydrate Formation

Huang Zeng,[†,‡] Lee D. Wilson[‡], Virginia K. Walker,[†] and John A. Ripmeester*[,†,‡]

Contribution from the Department of Biology, Queen's University, Kingston, Ontario K7L 3N6, Canada, and National Research Council of Canada, Ottawa, Ontario K1A 0R6, Canada

Received July 18, 2005; E-mail: john.ripmeester@nrc-cnrc.gc.ca

Abstract: The inhibition activities of two antifreeze proteins (AFPs) on the formation of tetrahydrofuran (THF) clathrate hydrate have been tested. AFPs from fish (wfAFP) and insect (CfAFP) changed the morphology of growing THF hydrate crystals. Also, both AFPs showed higher activities in inhibiting the formation THF hydrate than a commercial kinetic inhibitor, poly(vinylpyrrolidone) (PVP). Strikingly, both AFPs also showed the ability to eliminate the "memory effect" in which the crystallization of hydrate occurs more quickly after the initial formation. This is the first report of molecules that can inhibit the memory effect. Since the homogeneous nucleation temperature for THF hydrate was measured to be 237 K, close to that observed for ice itself, the action of kinetic inhibitors must involve heterogeneous nucleation. On the basis of our results, we postulate a mechanism for heterogeneous nucleation, the memory effect and its elimination by antifreeze proteins.

Introduction

Clathrate hydrates are crystalline, ice-like solids that form when guest molecules (4−8 Å) are trapped in frameworks formed by hydrogen-bonded water molecules.[1] In the petroleum industry, natural gas hydrate plugs formed during production, transportation and processing have long been a serious problem.[2] Some chemicals, like methanol, can shift the hydrate equilibrium conditions such that the operational conditions fall outside the hydrate formation region. They are called thermodynamic inhibitors. Recently, new groups of chemical inhibitors have been developed that act in a different way. Some, such as the "anti-agglomerants", keep small hydrate particles dispersed as they form[3] and other "kinetic inhibitors" retard hydrate formation to times that are longer than the residence time of the gas in the pipeline.[4] Kinetic inhibitors are polymer-based and likely cause interference with the nucleation and/or the crystal growth of hydrate. The effective concentrations of these new types of inhibitors are much lower than those required for thermodynamic inhibitors.

Antifreeze proteins (AFPs) and antifreeze glycoproteins (AFGPs) are found in certain cold-adapted organisms.[5] They can bind to embryonic ice crystals and prevent their growth within a certain temperature range and, consequently, depress the freezing point of body fluid in a noncolligative manner.[6] The inhibition activity has been proposed to derive from the Kelvin effect induced by the adsorption of AFPs on the ice surface, and is referred to as the adsorption-inhibition hypothesis.[7] Several types of AFPs and AFGPs have been identified from cold-water fishes, and one group of these, Type I AFPs from winter flounder and sculpin are small, α-helical, Ala-rich proteins.[5] AFPs with a β-helical, Thr- and Cys-rich structure have been isolated from insects.[8,9] Their ice growth inhibition activity can be up to 100 times higher than that of the fish AFPs on a molar basis,[10] although it is not yet understood how such high activity is achieved (but see ref 11). The proposed mechanism for AFP activity has led us to question whether AFPs can inhibit the formation of clathrate hydrate and this has been explored by examining the inhibition activity of fish and insect AFP on tetrahydrofuran (THF) hydrate and by comparison with the kinetic inhibitor, poly(N-vinylpyrrolidone) (PVP).

[†] Queen's University.
[‡] National Research Council of Canada.

(1) Sloan, E. D., Jr. *Clathrate Hydrates of Natural Gases*, 2nd ed.; Marcel Dekker: New York, 1998.
(2) Mehta, A. P.; Klomp, U. C. *Proceeding of 5th International Conference on Gas Hydrates*; 2005; *4*, 1089−1100.
(3) Lederhos, J. P.; Long, J. P.; Sum, A.; Christiansen, R. L.; Sloan, E. D., Jr. *Chem. Eng. Sci.* **1996**, *51* (8), 1221−1229.
(4) Sloan, E. D., Jr. US Patent No. 5,432,292, 1995.
(5) Davies, P. L.; Baardsnes, J.; Kuiper, M. J.; Walker, V. K. *Philos. Trans. R. Soc. London B Biol. Sci.* **2002**, *357*, 927−933.
(6) Yeh, Y.; Feeney, R. E. *Chem. Rev.* **1996**, *96*, 601−618.
(7) Raymond, J. A.; DeVries, A. L. *Proc. Natl. Acad. Sci. U.S.A.* **1977**, *74*, 2581−2593.
(8) Tyshenko, M. G.; Doucet, D.; Davies, P. L.; Walker, V. K. *Nat. Biotechnol.* **1997**, *15*, 887−890.
(9) Graham, L. A.; Liou, Y. C.; Walker, V. K.; Davies, P. L. *Nature* **1997**, *388*, 727−728.
(10) Walker, V. K.; Kuiper, M. J.; Tyshenko, M. G.; Doucet, D.; Graether, S. P.; Liou, Y. C.; Sykes, B. D.; Jia, Z. C.; Davies, P. L.; Graham, L. A. In *Insect Timing: Circadian Rhythmicity to Seasonality*; Denlinger, D. L., Giebultowicz, J., Saunders, D. S., Eds.; Elsevier: Amsterdam, 2001; Chapter 16, pp199−211.
(11) Wathen, B.; Kuiper, M.; Walker, V. K.; Jia, Z. C. *J. Am. Chem. Soc.* **2003**, *125*, 729−737.

10.1021/ja0548182 CCC: $33.50

Experimental Section

1. Materials. Purified fish Type I AFP from winter flounder (wfAFP; 4000 Da) was kindly provided by A/F Protein Canada Inc. An inactive form of wfAFP with a Leu for Ala substitution at position 17 (A17L) was chemically synthesized at the Queen's University Protein Function Discovery facility. Recombinant AFP from the spruce budworm insect, *Choristoneura fumiferama*, (CfAFP; 9000 Da) was produced as previously described.[10] Cytochrome C (12 000 Da) and bovine serum albumin (BSA; 67 000 Da) were purchased from Aldrich Inc. (Canada). Poly(N-vinylpyrrolidone) (PVP−K30, molecular mass ∼40 000) was kindly provided by Dr. E. D. Sloan (Colorado School of Mines, Golden, CO).

Silicone oil AR20 from Fluka (Switzerland) was used for the emulsion experiments. The surfactant, SP65, was from Sigma (Canada). THF and water of HPLC grade were obtained from Fisher Scientific (Canada).

2. Methods. 2.1. Preparation of THF Hydrate. THF hydrate was prepared by using a mixture of THF/water at a molar ratio of 1:15. Although THF and water form a hydrate at a molar ratio of 1:17 that melts congruently at 277.4 K (1 atm.), preliminary differential scanning calorimetry (DSC) measurements (not shown) indicated that a mixture of ice and THF hydrate was usually obtained by cooling a stoichiometric (1:17) solution. Therefore, a slight excess of THF (1:15) was used to ensure that the crystals obtained were pure THF hydrate.

For observation of THF hydrate crystal growth, an apparatus was constructed according to a published design.[12,13] A THF-water (1:15 molar ratio) solution was placed inside a glass tube and cooled below the hydrate melting point (275.5 K). A copper wire, cooled with dry ice, inserted into a glass pipet, was placed in the tube to initiate hydrate formation as a single crystal at the tip of the pipet. The resulting hydrate crystal was transferred into the THF−H_2O test solutions (containing proteins or PVP) and kept at 275.5 K. The time-dependent growth of the crystal was monitored with a HITACHI video camera (HV-62C) equipped with an OPTEM macro video zoom lens (18 to 108 mm) and images were captured with an ATI graphics card (ATI TV Wonder VE).

2.2. Induction Time Measurement. Induction time was assessed in an apparatus containing 14 test tubes with a small stirring bar and 3 mL of test solution immersed in a tank containing circulating coolant at 273.0 or 274.0 K.[12] The onset of hydrate formation was indicated by a sudden temperature increase of several degrees in the sample, as monitored by thermocouples, connected to a data acquisition board (OMEGA DBK52). The induction time is defined as the difference between the onset of hydrate formation and the time at which the test solution reached the bath temperature (Figure 1). If hydrates were not formed after 24 h, the induction time was arbitrarily assigned as >24 h. Approximately 50 induction time data points were collected for each sample, and the percentage of unfrozen samples vs time was used to assess inhibition activities. Samples tested included THF solutions and THF solutions containing cytochrome C, BSA, wfAFP, CfAFP, or PVP.

2.3. Homogeneous Nucleation Temperature Measurement. The homogeneous nucleation kinetics of THF hydrate were assayed by DSC on sample solutions (0.2 mg) emulsified in silicone oil as previously described for ice nucleation experiments.[14] Since THF has some solubility in silicone oil, sufficient THF was added to give the correct THF concentration in emulsified water droplets. The dispersed aqueous droplets were cooled at 1.0 K/min.

Results and Discussion

1. Morphological Observations of THF Hydrate Crystals. Single crystals of THF hydrate were successfully grown at the end of a glass pipet at 275.5 K and grew into regular octahedra (Figure 2A). However, if the crystal, while still small, was transferred to a THF solution containing 0.05 mM wfAFP, octahedral crystal growth was inhibited and only platelike crystal growth was observed (Figure 2C), similar to the growth observed in PVP-containing solutions (Figure 2B). The hyperactive AFP from CfAFP, also showed similar, slow platelike growth (Figure 2D), as seen with wfAFP and PVP. When hydrate crystals were transferred to THF solutions containing 0.05 mM BSA, the octrahedral crystals could not be distinguished from those grown in THF solutions alone (not shown).

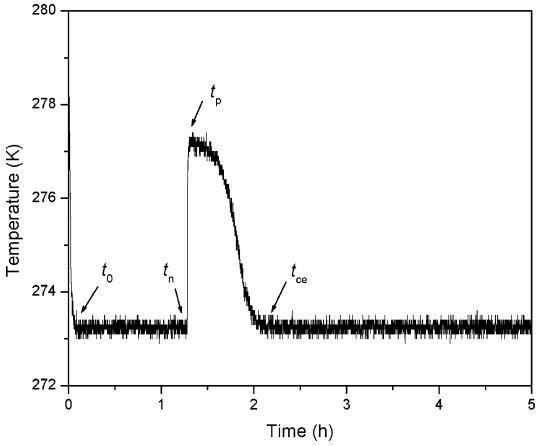

Figure 1. Typical exothermal peak recorded during the induction time measurement for the THF hydrate formation from THF−H_2O. Symbols include t_0: the time when the sample reaches the bath temperature; t_n: the time when nucleation starts, indicated by a sudden temperature increase; t_p: the time when the sample attains peak temperature (277 K); t_{ce}: the time when the crystallization ends and the temperature drops to the bath temperature. The induction time, t_i, is defined as $t_i = t_n - t_0$.

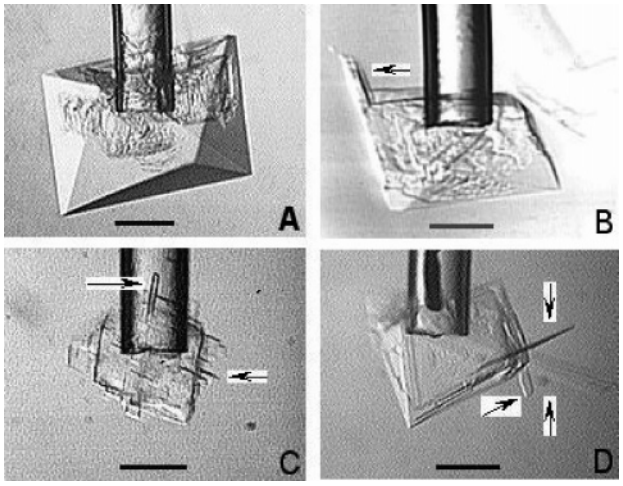

Figure 2. Morphology of THF hydrate crystal growth: (A) octahedral THF crystals (B) platelike THF crystal growth in the presence of 0.05 mM PVP, (C) 0.05 mM wfAFP and (D) 0.05 mM CfAFP. The images were captured about 5 min after transfer to the testing solution. The length of the bar is 1.3 mm and the platelike crystals that appeared and grew out from original octahedral crystal are marked with arrows.

2. Induction Time Measurements. A typical curve for the induction time for hydrate formation is shown in Figure 1. In the plot, t_0 is the time when the sample reaches the bath temperature; t_n is the time when the nucleation starts and is indicated by a sudden temperature increase; t_p represents the time when the sample attains peak temperature (∼277.0 K); and t_{ce} is the time when the crystallization ends and the

(12) Zeng, H.; Wilson, L. D.; Walker, V. K.; Ripmeester, J. A. *Can. J. Phys.* **2003**, *81*, 17−24.
(13) Makogon, T. Y.; Larsen, R.; Knight, C. A.; Sloan, E. D., Jr. *J. Cryst. Growth* **1997**, *179*, 258−262.
(14) Michelmore, R. W.; Franks, F. *Cryobiology* **1981**, *19*, 163−171.

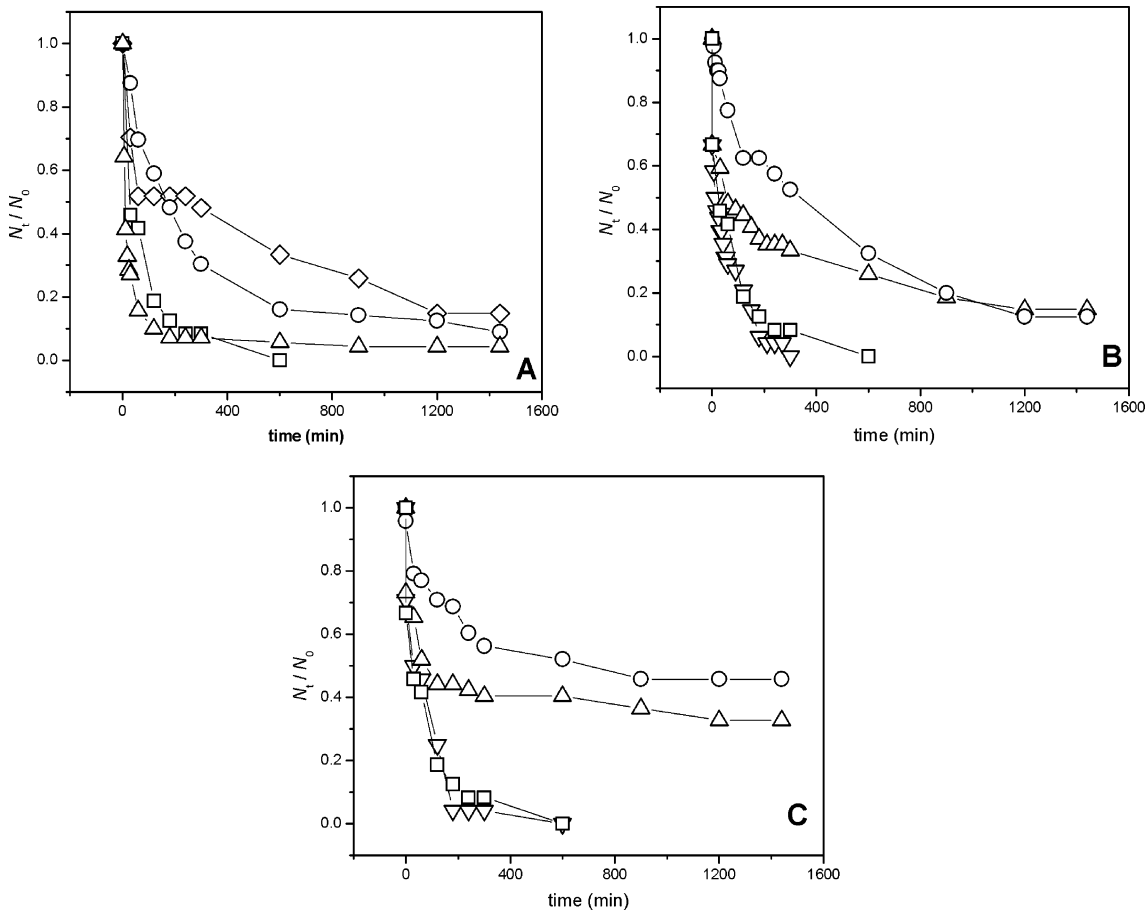

Figure 3. Induction effects of different additives at 0.05 (A), 0.14 (B), and 0.25 mM (C) on the formation of THF hydrate at 273 K. N_t: number of unfrozen samples at time t; N_0: number of unfrozen samples at the starting time (N_0 is about 50 for all the samples). □: THF−H_2O; ○: wfAFP−THF−H_2O; ◇: CfAFP−THF−H_2O; △: PVP-THF−H_2O; ▽: cytochrome C−THF−H_2O; Note that CfAFP was only tested at 0.05 mM (A).

temperature drops to the bath temperature. The induction time, t_i, is defined as

$$t_i = t_n - t_0$$

and was used to compare THF hydrate formation under different conditions and in different samples as follows.

2.1. The Effect of Proteins and PVP on the Formation of THF Hydrate. The effects of AFPs, control proteins and PVP, on the induction time for hydrate formation at 273 K are shown in Figure 3. N_t represents the number of samples that had not formed hydrates (assessed by induction time, t_i) at time t, and N_0 is the number of samples (∼50). Therefore, N_t/N_0 (i.e., the uncrystallized fraction) vs. time represents the inhibition activity of the additive. In effect, the slower the curve declines, the stronger the inhibition. Most curves could be fit reasonably well by first-order kinetics once the samples which did not form hydrate were accounted for. That is, the fraction of samples with hydrate N_t/N_0 varied as a function of time as

$$N_t/N_0 = (1 - A) + A \exp(-t/t_1)$$

where A was the fraction of samples that showed hydrate formation during the entire observation period (independent of lag time, t_1). The fitting results are represented in Figure 4 and listed in the Supporting Information. The large error bars for some of the inhibited samples indicate that first-order kinetics may not be an ideal description of the process but this does not change the general conclusions. The known kinetic inhibitor, PVP, inhibited hydrate formation as a function of concentration. At 0.05 mM, PVP did not show inhibition activity to the THF hydrate formation. After 300 min, more than 90% of the PVP−THF−H_2O samples had crystallized (Figure 3A). For PVP at 0.14 mM, 65% of the tubes had crystallized after 300 min (Figure 3B) compared with 90% of the control (THF−H_2O) tubes. PVP at 0.25 mM showed significant inhibition activity and about 40% of the samples remained hydrate-free after 300 min (Figure 3C). Strikingly, wfAFP showed stronger inhibition activity than PVP at every concentration used. For example, at 0.14 mM wfAFP, less than 50% of the samples had crystallized after 300 min. Although the availability of CfAFP was limited, it also showed strong inhibition activity, with similar induction times for 0.05 mM CfAFP as seen for 0.14 mM wfAFP (Figure 3A,B). In contrast, at the same concentration or higher, the control protein, cytochrome C, showed no inhibition (Figure 3B,C).

2.2. The Reformation of THF Hydrate: the Memory Effect. If the THF solutions were crystallized and then melted before subjecting the samples to low temperature again, hydrate formation was accelerated, compared to fresh solutions, suggesting a "memory effect" (Figure 5). The reformation of hydrate was tested when THF solutions were recrystallized at 273.0 K (Figure 5A) or 274.0 K (Figure 5B). These experiments also indicated that the rate of reformation was influenced by the temperature at which the melted hydrate was kept prior to

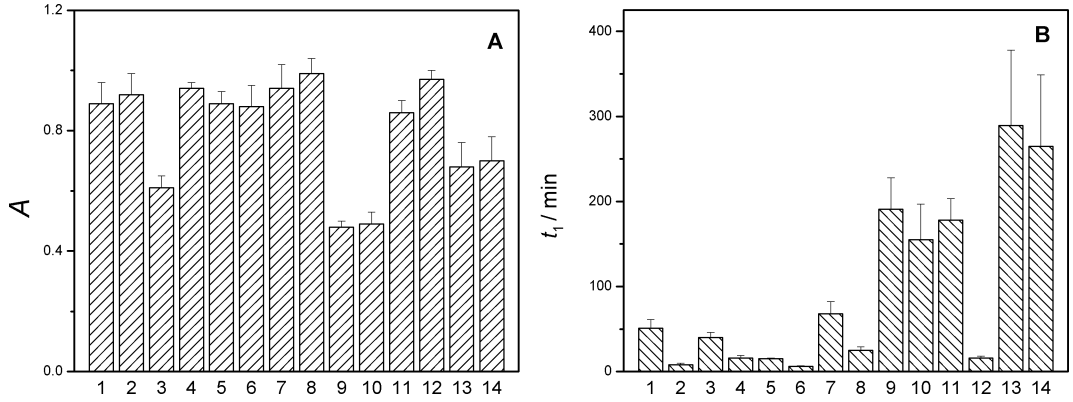

Figure 4. Fitting results for THF hydrate formation in bulk solution at 273 K. A shows the fraction of samples that showed hydrate formation during the observation period (*A*), independent of lag time, and B hydrate formation after the average lag time, t_1: Samples: 1: THF−H_2O; 2: THF−H_2O, melted (at 279.5 K for 1h before isothermal at 273 K; see text) and THF−H_2O solutions with additives: 3: PVP (0.25 mM); 4: PVP (0.25 mM), melted; 5: PVP (0.05 mM); 6: PVP (0.05 mM), melted; 7. cytochrome C (0.25 mM); 8: cytochrome C (0.25 mM), melted; 9: wfAFP (0.25 mM); 10: wfAFP (0.25 mM), melted; 11. wfAFP (0.05 mM); 12: wfAFP (0.05 mM), melted; 13. CfAFP (0.05 mM); 14: CfAFP (0.05 mM), melted.

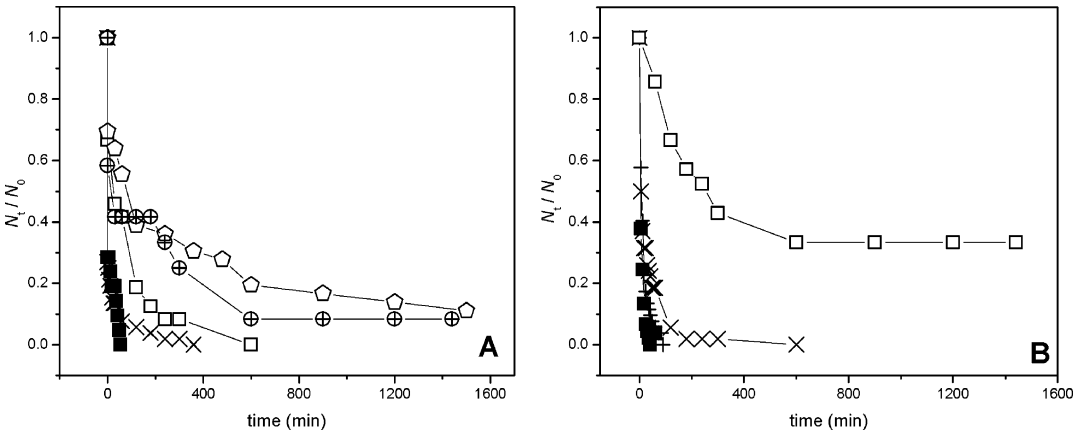

Figure 5. Effect of pretreatment temperature on the induction time of THF hydrate, or the memory effect. (A) isothermal at 273.0 K and (B) isothermal at 274.0 K. Samples were ■: melted at 279.5 K 1 h; +: melted at 281.5 K 1 h; ×: melted at 283.5 K 1 h; □: melted at 298.0 K 1h; ⊕: melted at 279.5 K 24 h; ⬠: all fresh samples.

recrystallization. Generally, the higher the temperature used for melting or the longer the time the sample was held at this temperature, the slower the reformation, but storage at 279.5 K for 24 h or 298.0 K for 1 h, still resulted in faster crystallization than in freshly prepared THF solutions. It is noted that there was no correlation between induction times within each system; the first samples to nucleate with freshly prepared solutions were not likely the first ones to nucleate after the thaw-freeze cycle. As well, samples that nucleated after a long lag time, initially, might nucleate faster when the temperature was lowered again.

There was no effect of PVP or a control protein on the memory effect observed after holding the THF solutions with these macromolecules at 279.5 K for 1 h before the samples were transferred to isothermal conditions at 273 K (Figure 6A). However, the addition of wfAFP or CfAFP to the THF solutions resulted in a concentration-dependent effect on hydrate reformation (Figure 6B). At a temperature about 2 K above the melting point of THF hydrate (i.e., 279.5 K), 0.25 mM wfAFP eliminated the memory effect while the presence of 0.05 mM wfAFP appeared relatively ineffective. In contrast, 0.05 mM CfAFP showed a strong effect on the reformation of THF hydrate and approached that of 0.25 mM wfAFP.

2.3. Comparison of wfAFP and the wfAFP A17L Mutant. An inactive form of wfAFP, A17L, showed an even stronger ability to inhibit the formation of THF hydrate than wfAFP, at the same concentration. After 300 min at 273 K and a concentration of 0.05 mM, 38% of the samples containing A17L had crystallized compared to 70% of the tubes containing wfAFP (Figure 7). Indeed, A17L showed an inhibition as strong as that seen with CfAFP (Figures 3 vs 7). However, THF hydrate reformed more quickly after a melt indicating that the mutant could not eliminate the memory effect (Figure 7).

3. Homogeneous Nucleation of THF Hydrate. In an attempt to clarify the inhibition mechanism, nucleation of THF hydrate formation was examined in droplets formed by emulsification. According to Michelmore and Franks,[14] the nucleation rate, J (nuclei $s^{-1}m^{-3}$) is expressed by

$$J = -\frac{1}{\upsilon t}\ln(N/N_0) \qquad (1)$$

where υ is the average volume of the droplet. N_0 is the total number of droplets at time 0, and N is the number of unfrozen droplets at time t. In this study, since the average droplet diameter was 2.0 μm, a volume of 4×10^{-18} m^3 was used to calculate nucleation kinetics. The value of N/N_0 can be achieved by using A/A_0 where A is the integrated peak area from the starting point of the peak to time t (temperature T), and A_0 is the total peak area, as shown in Figure 8A. Thus, the nucleation

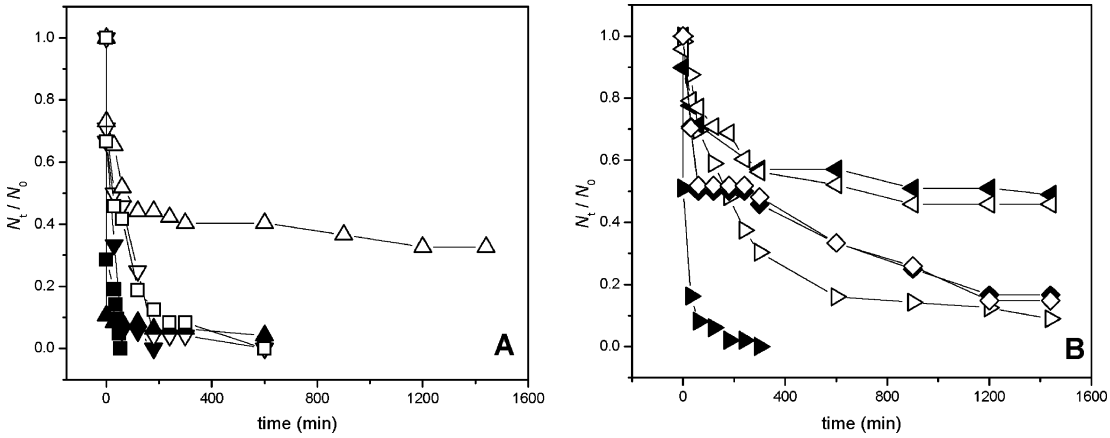

Figure 6. Effects of different additives (A for control macromolecules and B for wfAFP) on the memory effect in THF hydrate formation. (melted at 279.5 K 1 h before isothermal recrystallization at 273.0 K). Samples were □: THF−H_2O; ■: THF−H_2O (melted); △ PVP (0.25 mM); ▲: PVP (0.25 mM, melted); ▽: cytochrome C (0.25 mM); ▼: cytochrome C (0.25 mM, melted); left-facing hollow triangle: wfAFP (0.25 mM); left-facing solid triangle: wfAFP (0.25 mM, melted); right-facing hollow triangle: wfAFP (0.05 mM); right-facing solid triangle: wfAFP (0.05 mM, melted); ◇: CfAFP (0.05 mM); ◆: CfAFP (0.05 mM, melted)

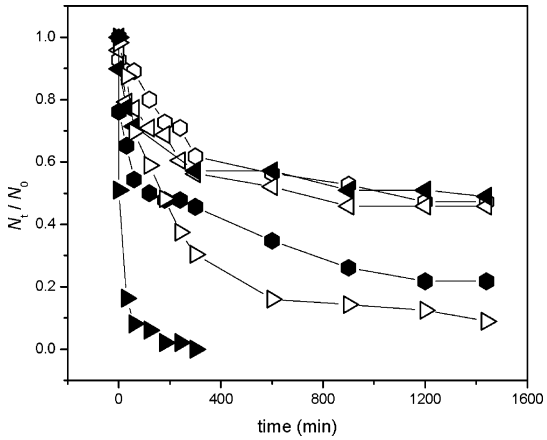

Figure 7. Comparison of the effects of wfAFP and A17L on the induction time and memory effect in THF hydrate formation (isothermal recrystallization at 273.0 K; or melted at 279.5 K 1h before isothermal recrystallization at 273.0 K). Left-facing hollow triangle: wfAFP (0.25 mM); left-facing solid triangle: wfAFP (0.25 mM, melted); right-facing hollow triangle: wfAFP (0.05 mM); right-facing solid triangle: wfAFP (0.05 mM, melted); hollow hexagon: A17L (0.05 mM); solid hexagon: A17L (0.05 mM, melted).

rate, J, can be expressed as a function of reduced temperature, θ, according to

$$J = A \exp(k\tau_\theta) \qquad (2)$$

where A and k are constants, τ_θ is function of reduced temperature, θ: $\tau_\theta = [\theta^3(\Delta\theta)^2]^{-1}$, with $\theta = T/T_m$, and $\Delta\theta = (T_m - T)/T_m$, where T is the temperature and T_m is the equilibrium melting temperature of THF hydrate. A typical curve showing the relationship between the nucleation rate, J, and τ_θ is shown in Figure 8B. There were only minor effects on the homogeneous nucleation of THF hydrate by PVP or the control protein; the maximum nucleation rate corresponded to a temperature of 237 K in each trial (Table 1). However, wfAFP increased the nucleation temperature (the temperature at which the nucleation rate reached a maximum value) by about 1 K while CfAFP tended to weakly inhibit it, as shown by a slight decrease in the nucleation temperature. In these small droplets, evidence of the memory effect seemed to disappear after the samples were heated for one min to 279.5 K, just 2 K above the THF hydrate melting point (Table 1). It is noted that the partitioning of THF between THF−H_2O solution and oil phase might change as the temperature was changed, but since this effect is expected to be the same for all the samples, it was not studied. Although it is a formal possibility that inhibitors could also change the partition ratio, the additives were present in such low concentrations (0.1−1 wt %) that it is unlikely.

Despite the interest in gas hydrate inhibition, it is still unclear if commercially important kinetic inhibitors are primarily hydrate growth inhibitors or nucleation inhibitors. The change in the morphology of the growing THF hydrate crystals by AFPs (Figure 2), which is similar to the effect seen with PVP (ref 13; Figure 2B), indicates that both types of macromolecules effectively inhibit hydrate growth. Whereas it took less than 5 h to form crystals in 90% of the THF solutions, with or without control proteins, not even 50% of the samples had crystallized in the presence of 0.25 mM PVP or wfAFP in the same period (Figure 3C). WfAFP showed concentration-dependent inhibition activities at all the three concentrations tested. In contrast to PVP, which was ineffective as an inhibitor at 0.05 mM, CfAFP at this low concentration had inhibition activities similar to that observed for wfAFP at 0.14 mM. These results indicate that wfAFP and CfAFP were considerably more effective at suppressing hydrate nucleation than the commercial inhibitor PVP.

AFPs are believed to decrease the growth of ice crystals by an adsorption-inhibition mechanism of inhibition. We suggest that AFPs can also inhibit hydrate growth by the same mechanism. AFPs are adsorbed onto tiny hydrate crystals or, alternatively, on impurity particles (that are unavoidable in bulk solutions) and effectively increase the energy barrier for further growth of the hydrate, or coat the surface of nucleating impurities thus making it difficult for heterogeneous nucleation to occur. It is curious that the mutant wfAFP, A17L, with no inhibition activity toward ice, was able to inhibit THF hydrate formation (Figure 7). It suggests that, unlike the requirements for ice inhibition, the Ala residue may not be crucial for adsorption to hydrates. In this regard, it is interesting to note that overall A17L was not as effective an inhibitor as wfAFP since the mutant did not inhibit the rapid reformation of hydrate demonstrated by the memory effect experiments.

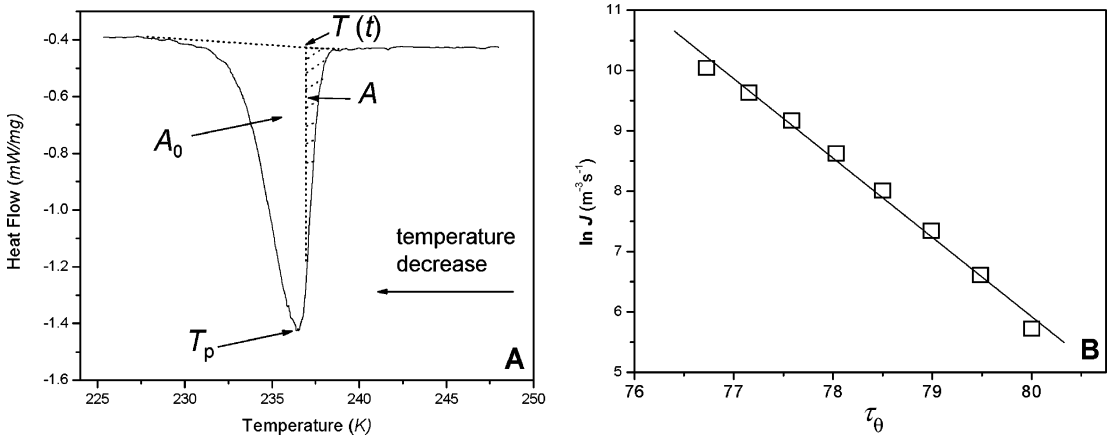

Figure 8. Homogeneous nucleation in emulsions of THF hydrate.(A) A typical DSC curve representing the freezing of the emulsion of THF−H_2O solution under constant cooling. T_p is the temperature at which the nucleation rate reached a maximum value. The heat of crystallization released at time t (temperature T), A, is represented by the shadow and A_0, the total peak area, represent the total heat of crystallization. (B) A typical curve showing the dependence of nucleation rate, J, and a function of reduced temperature, τ_θ.

Table 1. Homogeneous Nucleation Data for Hydrate-forming Solutions[a]

hydrate type	T_p (K)[b]	ln A (m^{-3} s^{-1})[c]	k[d]
THF	237.1 ± 0.2	67.2	−0.72
melted at 279.5 K 1 min	236.5 ± 0.6		
THF-cyto C (0.25 mM)	237.2 ± 0.2	70.4	−0.76
THF-PVP (0.25 mM)	237.2 ± 0.2	68.1	−0.74
THF-wfAFP (0.25 mM)	238.0 ± 0.3	57.0	−0.57
THF-CfAFP (0.25 mM)	236.6 ± 0.2	79.7	−0.90

[a] Data are the average of at least three measurements on independent samples. [b] T_p is the temperature corresponding to the maximum nucleation rate. The mean droplet volume is taken as 4×10^{-18} m^3. [c] A: constant. [d] k: constant.

Hydrate crystallization has a well-recognized "memory" in that if hydrates crystallize from a solution and are melted, they can subsequently reform much more rapidly.[1,15−18] In pipelines, this can lead to the troublesome reformation of serious blockages after plugs have been decomposed[1]. Induction time measurements on once-melted THF solutions showed that wfAFP (0.25 mM) and even lower concentrations of CfAFP (0.05 mM) were effective at suppressing the reformation of hydrates. To our knowledge, this is the first report of molecules that can eliminate the memory effect.

The various observations allow us to postulate a mechanism for heterogeneous nucleation, the memory effect, and its elimination by AFPs. Since the homogeneous nucleation temperature lies far below the temperatures of the various events we study here, we must conclude that the memory effect operates in the realm of heterogeneous nucleation, that is, it involves impurities that act as nucleation sites. This observation eliminates so-called "structural" memory effects, that is those due to residual hydrate structure in solution that persists after melting of the hydrate.[1,15,19] This would be an intrinsic property, hence it should still be observable in the small droplets used for the homogeneous nucleation experiment, where in fact no memory effects were observed (Table 1).

Therefore, when AFPs act as inhibitors of primary nucleation, this must mean that they adsorb to the impurity particle surfaces thus blocking the nucleating sites on these particles. The memory effect improved heterogeneous nucleation during hydrate reformation, therefore must be ascribed to an alteration of the surface states of the impurity particles that amplifies their nucleating action. This could occur because of an imprinting of the surface of the impurities by the growth of a hydrate crystal on the particle surfaces. For instance, if the impurities are hydrated or hydroxylated silicon or iron oxides, a hydrate crystal may well alter the surface geometry so that when the hydrate melts, the surface is now a better nucleator of hydrate than it was during the first nucleation cycle. Contact with the aqueous solution will allow the surface to relax to its original state, thus giving the memory effect a finite lifetime which depends both on temperature and time, as observed. The AFPs can eliminate the memory effect by adsorbing to the altered particle surfaces, which may well be stronger adsorbers of AFPs than during the first nucleation cycle.

The characteristics of the various kinetic inhibitors, e.g., as modifiers of hydrate growth, as inhibitors of initial hydrate nucleation or hydrate re-nucleation all can be classified systematically and suggest that in the future that kinetic inhibitors may be designed according to their specific activity in the different phases of hydrate formation.

Further work is needed to relate specific structural properties of the AFPs (e.g. the α-helix for wfAFP and β-helix for CfAFP) to their effectiveness in inhibiting heterogeneous nucleation or growth of hydrate. As mentioned before, one can assume that in general all macromolecules adsorb on surfaces to a certain extent, so one must look for differences in adsorption strength or the type of adsorbed film that is formed. Whether this involves surface matching of the protein structure to the hydrate crystal planes via a variety of interactions, as has been proposed for ice[5,20] is a moot point, as this does not necessarily explain the activity of AFPs in inhibiting heterogeneous nucleation, for instance, by adsorbing to impurity particle surfaces. It is now known that AFPs also adsorb on calcite[21] and on silica[22] and

(15) Takeya, S.; Hori, A.; Hondoh, T.; Uchida, T. *J. Phys. Chem. B* **2000**, *104*, 4164−4168.
(16) Ohmura, R.; Ogawa, M.; Yasuoka, K.; Mori, Y. H. *J. Phys. Chem. B* **2003**, *107*, 5289−5293.
(17) Servio, P.; Englezos, P. *Cryst. Growth Des.* **2003**, *3* (1), 61−66.
(18) Servio, P.; Englezos, P. *AIChE J.* **2003**, *49* (1), 269−276.
(19) Rodger, P. M. *Ann. N. Y. Acad. Sci.* **2000**, *912*, 474−482.
(20) Yang, C.; Sharp, K. A. *Proteins: Struct., Funct. Bioinform.* **2005**, *59*, 266−274.
(21) DeOlivera, D.; Laursen, R. *J. Am. Chem. Soc.* **1997**, *119*, 10627−10631.
(22) Zeng, H. Ph.D. Thesis, Queen's University, Canada, 2004.

that they also inhibit the formation of sI hydrate,[22] all very different surfaces, the common factor being that they are hydrophilic. These various observations suggest that the actual inhibition mechanism for ice and hydrate growth needs to be reexamined. Perhaps new insight may be gained from modeling studies. No matter the actual mechanism, the ability of protein antifreezes to inhibit both hydrate formation and the memory effect has important prospects for both utility and safety. We have shown that inhibition of nucleation and growth of hydrates are quite separate processes, with the first extrinsic and related to impurities, whereas the second is related directly to the interaction of the inhibitors with hydrate crystals. Hence, AFPs may serve as models for the design of new materials with improved and specific inhibiting activity toward hydrates.

Conclusion

AFPs from fishes and insects change the crystal habit of THF hydrate, and also inhibit hydrate crystal growth. Since the homogeneous nucleation temperature is lower than the usual crystallization temperatures we have shown that kinetic inhibitors work in the realm of heterogeneous nucleation and the AFPs have higher inhibition activities toward THF hydrate than the commercial kinetic inhibitor, PVP. Active AFPs also inhibit the faster reformation, or memory effect, of THF hydrate, but an ice-inactive mutant did not, suggesting that some aspects of the mechanism of ice growth adsorption-inhibition are shared with this hydrate inhibition phenomenon. Whatever the reason, inhibitors based on AFPs are likely to find utility in the prevention of unscheduled hydrate growth.

Acknowledgment. We thank A/F Protein Canada Inc. (Dr. G. Fletcher and Dr. S. Goddard) for providing the Type I AFP and Dr. E. D. Sloan for the PVP. We also thank these scientists, as well as Dr. M. Kuiper for encouragement. Queen's University Protein Function Discovery facility is acknowledged for the chemical synthesis of the AFP mutant. The NSERC/NRC/Industry partnership program is acknowledged for a grant to V.K.W. and J.A.R. Partial support for H.Z. was provided by a Queen's University graduate scholarship.

Supporting Information Available: Fitting parameters for the kinetic curves for the crystallization runs. This material is available free of charge via the Internet at http://pubs.acs.org.

JA0548182